Mutagenesis, 2018, 33, 195–202
doi:10.1093/mutage/gey012
Original Manuscript
Advance Access publication 20 July 2018

OXFORD

Original Manuscript

A novel *IRF6* mutation causing non-syndromic cleft lip with or without cleft palate in a pedigree

Huaxiang Zhao[1,†], Mengqi Zhang[1,†], Wenjie Zhong[1], Jieni Zhang[1], Wenbin Huang[1], Yunfan Zhang[1], Weiran Li[1], Peizeng Jia[1], Taowen Zhang[2], Zhonghao Liu[3], Jiuxiang Lin[1,*] and Feng Chen[4,*]

[1]Department of Orthodontics, Peking University School and Hospital of Stomatology, Beijing100081, PR China, [2]Department of Orthodontics, Yantai Stomatology Hospital, Shandong 264001, PR China, [3]Department of Oral Implantology, Yantai Stomatology Hospital, Shandong 264001, PR China and [4]Central Laboratory, Peking University School and Hospital of Stomatology, Beijing 100081, PR China

*To whom correspondence should be addressed. Tel: +86 10 82195336; Fax: +86 10 82195336; Email: jxlin@pku.edu.cn (Jiuxiang Lin). 22 Zhongguancun South Avenue, Haidian District, 100081 Beijing, PR China. Tel: +86 10 82195773; Fax: +86 10 82195773; Email: chenfeng2011@hsc.pku.edu.cn (Feng Chen)

†H. Zhao and M. Zhang contributed equally to this work.

Received 25 January 2018; Revised 1 May 2018; Editorial decision 5 June 2018; Accepted 6 July 2018.

Abstract

Non-syndromic cleft lip with or without cleft palate (NSCLP) is the most common congenital craniofacial malformation, and its harmful influence on affected individuals is apparent. Despite many studies, the causative genes and their mechanisms are not completely clear. We recruited a Han Chinese NSCLP family and explored the causative variant in this pedigree. We performed whole-exome sequencing on two patients. Bioinformatics screening and analysis were used to identify the mutation. We also performed species conservation analysis, mutation function predictions, and homology protein modelling to evaluate the influence of the mutation. We identified a rare mutation in interferon regulatory factor 6 (IRF6) (c.26G>A; p.Arg9Gln) as a candidate of causative mutation. This mutation was predicted to be deleterious. The codon is conserved in many species. The residue change caused by this mutation would affect the structure of IRF6 to a degree. Our study suggested that the rare *IRF6* variant is probably the pathogenic mutation in this family. Our result adds evidence that *IRF6* variants play a role in the aetiology of orofacial clefts.

Introduction

Cleft lip and/or palate (CLP) is the most common disruption of the normal facial structure. Worldwide, CLP affects approximately 1 in 700 live births. The prevalence varies geographically and ethnically and with environmental exposure and socio-economic status (1). Approximately 70% of the cases of CLP occur as isolated entities with no other apparent cognitive or craniofacial structural abnormalities; these are called non-syndromic cleft lip with or without cleft palate (NSCLP).

NSCLP imposes a substantial financial and social burden on patients and their families (1). NSCLP can cause problems with feeding, speaking, hearing, and social integration, and these can be corrected to varying degrees by surgery, dental treatment, speech therapy, and psychosocial intervention. Due to the complexity and specificity of the oral cavity with cleft palate, the treatment for such patients is very challenging.

Compared with syndromic CLP, NSCLP has a more complicated aetiology because of its genetic heterogeneity, the limited availability and high cost of genomic tools, and the need for collection of a very

large number of samples. With the advent of genomics tools, many studies have explored the aetiology of NSCLP. The combination of candidate genes (2) and genome-wide studies (3–5), plus the analysis of animal models (6–8), has provided deeper insight into the aetiology of NSCLP. With the development of inexpensive sequencing technology, whole-exome sequencing (WES) is playing an increasingly important role in studying the aetiology of hereditary diseases (9,10). Compared with genome-wide association studies (GWAS), the advantages of WES are obvious: it is more efficient, complete, and specific (6,7). Combining WES with GWAS should lead to a deeper understanding of the causes of NSCLP.

Interferon regulatory factor 6 (IRF6) belongs to a family of transcription factors that share a highly conserved N-terminal DNA-binding domain (DBD) and a less conserved C-terminal protein-binding Smad-interferon regulatory factor-binding domain (SMIR/IAD). *IRF6* variants were first identified as aetiological in the autosomal-dominant Van der Woude syndrome, which consists of cleft lip and palate with dental anomalies and lip fistulas (11). *IRF6* variants also contribute to the risk of NSCLP according to GWAS (5,12,13).

In this study, we examined a family with hereditary NSCLP. WES was performed on the affected members. Variants were screened according to their frequency, function, and position to identify the aetiological variant in this family. We also performed species conservation analysis, mutation function prediction, and homology protein modelling to evaluate the influence of the mutant allele.

Methods and materials

Participants

We identified a family with inherited NSCLP at the Peking University Hospital of Stomatology. Clinical information and peripheral blood samples were obtained from each recruited family member. Informed consent was obtained from each subject or his parents. This study and the associated research protocols were approved by the ethics committees of the Peking University Hospital of Stomatology (PKUSSIRB-201520012).

Clinical examinations and diagnoses were performed separately by a dentist and maxillofacial surgeon. Patients also underwent a complete physical examination to ensure that there were no other organ malformations or deformities. A detailed prenatal exposure history of the mother of the proband was collected, including smoking, drinking, disease history, medicine and supplement use, and exposure to radiation, poisons, and chemicals. A healthy family member was examined to eliminate the possibility of occult submucous CLP.

DNA extraction from blood samples

Genomic DNA was extracted from 400 µl peripheral blood using a QIAamp DNA Mini Kit (QIAGEN, Düsseldorf, Germany) following the manufacturer's instructions. The quality and quantity of the DNA samples were assessed using a NanoDrop 8000 (Thermo Scientific™, Waltham, MA, USA) and agarose gel electrophoresis (AGE).

Whole-exome sequencing

To identify the causative mutation, we performed WES on a BGISEQ-500 machine (BGI, China) (14).

The bioinformatics analysis began with the raw sequence data from the BGISEQ-500. First, clean data were produced by excluding adapter sequences and low-quality and undetected bases. The clean data for each sample were mapped to the human reference genome (GRCh37/HG19) using the Burrows–Wheeler Aligner (BWA) (Oxford, UK). To ensure accurate variant calling, we followed the recommended best practices for variant analysis with the Genome Analysis Toolkit (GATK, https://www.broadinstitute.org/gatk/guide/best-practices). Local realignment around indels and base quality score recalibration were performed using GATK. Duplicated reads were removed using Picard Tools (http://broadinstitute.github.io/picard/). The sequencing depth and coverage for each individual were calculated based on the alignments. SnpEff (http://snpeff.sourceforge.net/SnpEff_manual.html) was then used to perform annotation and prediction.

Screening the causative gene

We excluded variants with a minor allele frequency > 5% in public databases (the 1000 Genomes Project, http://www.1000genomes.org/) as well as variants in the non-coding DNA sequence, including the 3′-UTR, 5′-UTR, downstream, upstream, intergenic, and intron regions and non-coding exon variants.

Each variant was evaluated for the potential to contribute to the orofacial cleft (OFC) based on a single-gene Mendelian model. According to the variant annotation and prediction by SnpEff, low-impact variants and variants that could be found in the NCBI dbSNP database were screened out. The literature was reviewed for individual variants and candidate genes with potential significant relationships to the phenotype and possible deleterious effects on craniofacial structures.

Sanger sequencing with forward (5′-GCCTCCTGCCACCACT-3′) and reverse (5′-GGCTAGATTCCCTAGACCA-3′) primers designed using Primer5 ver. 0.4.0 was applied to the candidate variant. The Sanger sequencing product was separated using an ABI 3730 genetic analyser, and the data were analysed using Chromas V1.0.0.1.

Species conservation analysis

Single nucleotide polymorphisms (SNPs) were assessed for evolutionary conservation using the UniProt Browser (www.uniprot.org) and ClustalX2.1.

Mutation function predictions

For further screening, SIFT (http://sift.jcvi.org), PolyPhen-2 (http://genetics.bwh.harvard.edu/pph2/), and MutationAssessor (http://mutationassessor.org/r3/) were used to predict mutation function (15).

Homology protein modelling

To obtain more insight into the effects of the mutations on the molecular structure of IRF6, we created a homology model. The sequence of IRF6 was downloaded from NCBI (www.ncbi.nlm.nih.gov/protein). SWISS-MODEL (swissmodel.expasy.org) was used for the molecular simulation (16). For specificity, the first domain of IRF6 (IRF) was simulated. We used IRF3 (2pi0.1. D) as the template to create a model for wild-type residues 3–116 (identity 40.71%) and for mutant residues 3–116 (identity 39.29%). The program created one model in each simulation. PyMOL software was used for visualisation.

Results

Phenotypic descriptions of the NSCLP pedigree

We studied a three-generation Han Chinese family affected with NSCLP. The proband (D1) has a left cleft lip and palate, while

his mother (D2) has a cleft palate (Figure 1). His father (C1) was healthy. Both patients underwent detailed oral and general physical examinations. D2 has a crossbite, and both of her upper second incisors are congenitally absent. D1 and C1 do not have obvious malocclusion. We eliminated the possibility of systemic malformation, including eyes and vision, external ear morphology and audition, cranioskeletal development, the morphology of the other long bones, the neuromuscular and motor systems, the cardiovascular system, and external genitals. Both patients were diagnosed with NSCLP. The detailed oral and general physical phenotypes are listed in supplementary Table 1, available at *Mutagenesis* Online.

During the pregnancy, D2 was not exposed to diseases, smoking, alcohol, radioactivity, or chemical teratogens. There was no supplementation with folic acid, iron, or vitamin B_6 and no exposure to antibiotics.

A novel IRF6 mutation is identified as the candidate aetiological variant in this NSCLP pedigree

To discover the causative variation in this family, we performed WES of two DNA samples with an average of 282 915 715 raw base reads. After removing low-quality data, we obtained an average of 267 606 747 clean reads. The clean reads of each sample had Q20 = 95.35% and Q30 = 88.28%, indicating high sequencing quality. The mean sequencing depth at the target regions was 194.86-fold (Table 1).

We identified 120 902 single nucleotide variants and indels in D1 and 124 129 in D2. On average, there were 66155.5 heterozygous

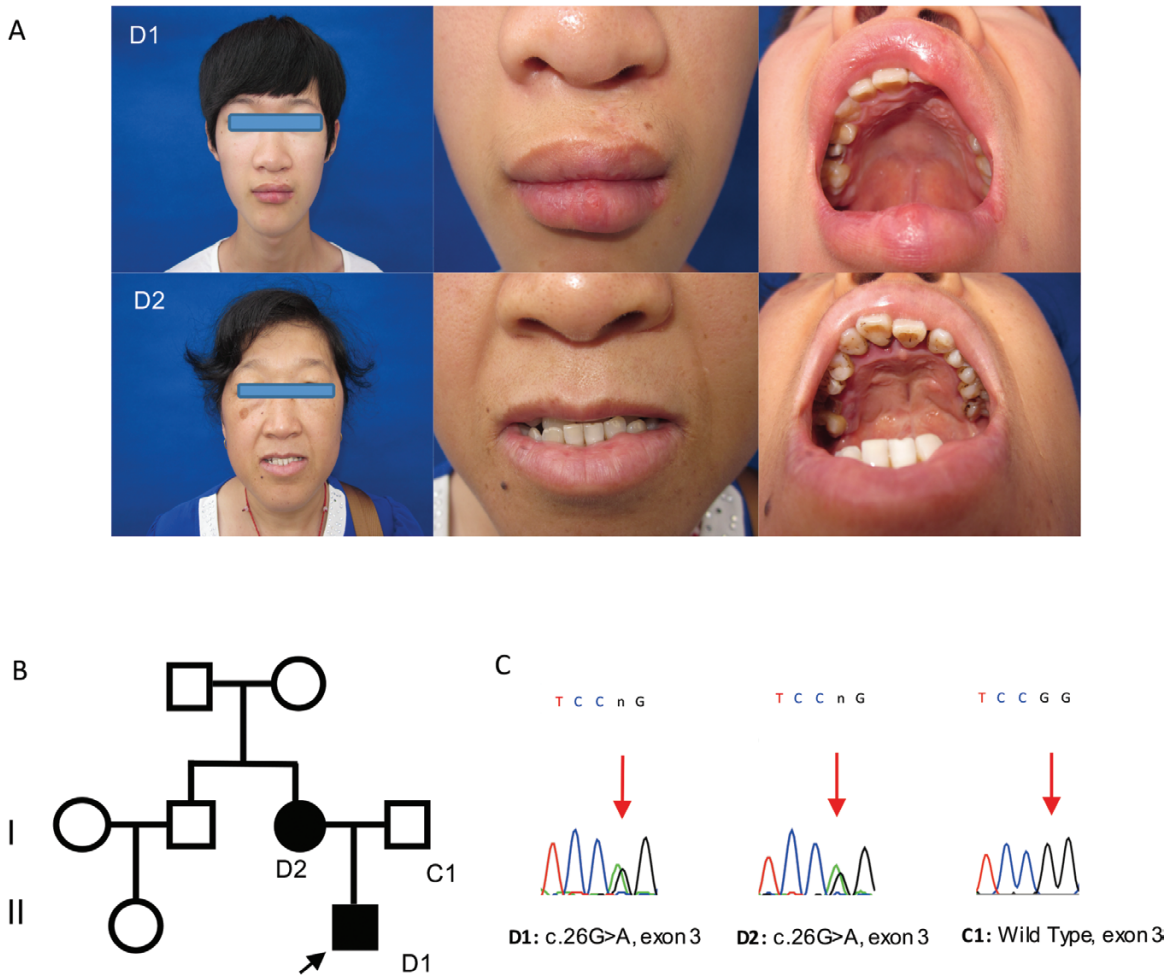

Figure 1. The pedigree information, phenotypes, and Sanger sequencing of the causative mutation in the NSCLP pedigree. (**A**, **B**)The proband (D1) is a man with left cleft lip and palate. Another NSCLP patient in this family, his mother (D2), had the same left cleft palate. The black arrow indicates the proband. (**C**) Sanger sequencing of the causative mutation. The mutations in D1 and D2 were heterozygous; C1 is the wild type. Red arrows indicate the position of causative variants.

Table 1. Summary of whole-exome sequencing data and alignment

Sample	Total effective yield (Gb)	Average sequencing depth	Q20%	Q30%	Mapping rate on genome (%)	Coverage of exome (%)	Target capture specificity (%)	Fraction of target covered ≥ 4× (%)	Fraction of target covered ≥ 20× (%)
D1	23.16	204.14	95.52	88.63	99.93	99.92	50.76	99.61	95.86
D2	23.31	185.58	95.17	87.93	99.93	99.77	45.84	99.51	96.86
Average	23.24	194.86	95.35	88.28	99.93	99.85	48.30	99.56	96.36

variants and 56 360 homozygous variants (Table 2). Both the quantity and quality of the sequencing met the requirements for further analysis.

After filtering out high-frequency variants, 19 618 and 20 234 variants remained in D1 and D2, respectively. After annotating the variants, we focussed only on nonsynonymous variants (NSVs) and indels in coding DNA sequences (CDS), which were more likely to be pathogenic than other variants. We favoured autosomal-dominant inheritance because of the family pedigree with an affected mother and son, although we considered all possible modes of inheritance when analysing the data. We selected the 1722 NSVs and indels that were shared by the two affected individuals. After removing those with low impact predicted by software, 1496 remained. Then, we selected those that were not found in the dbSNP database. The total number was 244. In supplementary Table 2, available at *Mutagenesis* Online, we chose the variants whose SIFT scores were smaller than 0.05 (deleterious) among the 244 variants. Finally, we examined reported genes with known roles in the pathogenesis of cleft lip and palate and eventually identified c.26G>A (NM_006147.3) in *IRF6* on chromosome 1, predicting p.Arg9Gln as the most likely candidate (Figure 2).

Using Sanger sequencing, we verified that the heterozygous mutation (c.26G>A) in *IRF6* (Figure 1) was present in the affected individuals (D1 and D2 in Figure 1) but not in the unaffected father.

The novel mutation is potentially deleterious

Multiple-sequence alignment of IRF6 showed that the residue Arg9 is evolutionarily conserved in all of the species compared, including *Homo sapiens*, *Mus musculus*, *Rattus norvegicus*, *Cavia porcellus*, *Pan troglodytes*, *Equus caballus*, *Papio anubis*, and *Oryctolagus cuniculus* (Figure 3C). In addition, several major algorithms predicted that the c.26G>A (p.Arg9Gln) mutation would cause disease. The SIFT score was 0.01 (deleterious score ≤ 0.05), the PolyPhen-2 score was 0.998 (deleterious score ≥ 0.909), and the MutationAssessor score was 2.2 (deleterious score ≥ 1.9) (Figure 3B); all were classified as potentially deleterious.

This missense mutation changed the wild-type codon 9 from CGG to CAG, replacing arginine with glutamine (p.Arg9Gln) in the IRF domain (Figure 3A) and thereby turning the positive charge of the residue side chain into a neutral charge. Homology modelling was performed based on the structure of the interferon-regulatory factor-3 DNA-binding domain (SMTL id: 2pi0.1. D) (Figure 4). In the mimetic structure of the first domain (IRF) of IRF6, differences were detected between the wild type and mutation: (i) the beta sheet at the beginning of wild-type IRF stopped at p.5, whereas the first beta sheet of the mutant IRF stopped at p.8, which is closer to the first alpha helix; (ii) because of the change in p.9, the orientation of the side chain of the ninth residue changed from vertical to the alpha helix to parallel; and (iii) the random coil between the

Table 2. Summary statistics for identified variants

Sample	Total variation	Heterozygotes	Homozygotes	Exonic	Intronic	Intergeneic	Splicing	Synonyomus	Missense	Stop-gain	Stop-loss
D1	120 902	65 295	55 607	39 689	81 213	3222	2274	11 026	10 429	95	37
D2	124 129	67 016	57 113	39 995	84 134	3438	2303	11 055	10 511	95	40
Average	122515.5	66155.5	56 360	39 842	82673.5	3330	2288.5	11040.5	10 470	95	38.5

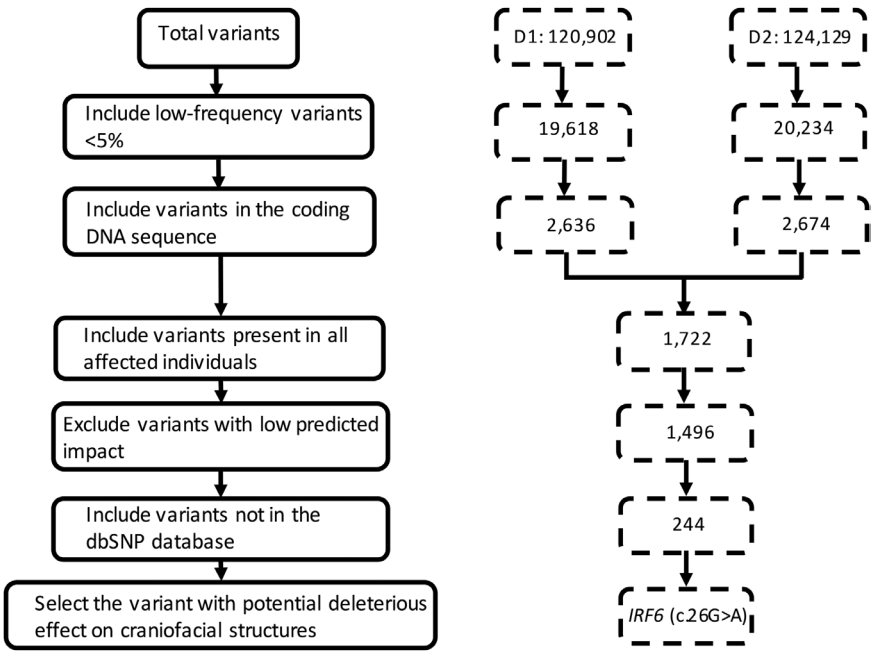

Figure 2. Flow chart outlining selection of the causative variant. The variants with high frequency (MAF > 5%) were excluded (19 618 variants in D1 and 20 234 variants in D2 remained). Variants in the CDS were included (2636 variants in D1 and 2674 variants in D2 remained). The variants shared by D1 and D2 were selected, which reduced the number of candidate genes to 1722. After excluding the variants with low predicted impact, 1496 variants remained. Including variants not in the dbSNP database, the literature on the individual variants and candidate genes was reviewed for potential significance related to the phenotype and possible deleterious effects on craniofacial structures.

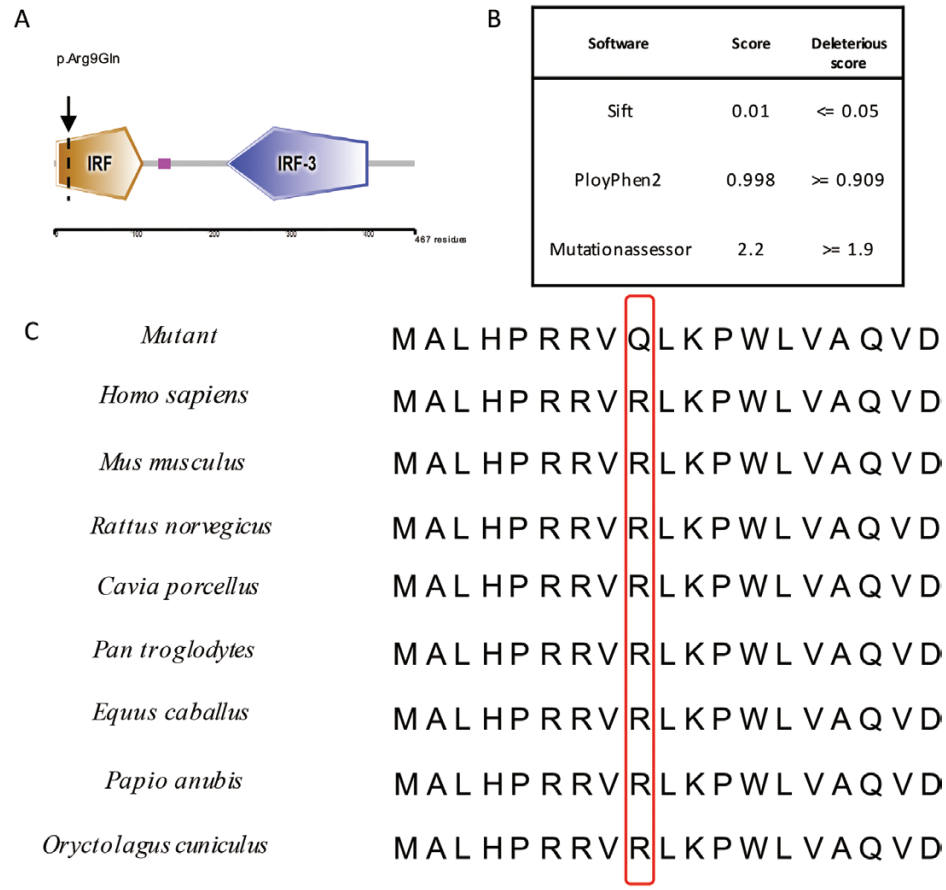

Figure 3. The position and conservation of the mutant protein. (**A**)The mutation was located in the first domain (IRF), p.Arg9Gln. (**B**)The predicted impact scores. (**C**) The residue Arg9 is evolutionarily conserved in *Homo sapiens, Mus musculus, Rattus norvegicus, Cavia porcellus, Pan troglodytes, Equus caballus, Papio anubis,* and *Oryctolagus cuniculus*.

second beta sheet and second alpha helix occupied p.42–p.56 in the wild-type IRF, while the random coil in the same position was longer and occupied p.40–p.57 in the mutant IRF; (iv) as shown in Figure 4C, we found that the electron-density distribution (electrostatic surface potential) differed between the mutant and wild-type proteins at the C-terminus. The area of negative potential seen in the mutant IRF6 model was shorter but higher than that of the wild-type one (Figure 4C).

Discussion

NSCLP is aetiologically heterogeneous (1). Its aetiology is complex, with both genetic and environmental contributions (17). The defects happen in early embryological development. Researchers are striving to identify the aetiological variants at novel loci to understand the developmental causes of NSCLP, which should eventually result in improved prevention, treatment, and prognosis for affected individuals.

Through GWAS and other research, some genetic risk factors have been discovered, but these explain only a part of the causes of NSCLP (18). To explore the aetiological variants of NSCLP, we performed WES in a family with inherited NSCLP. After screening and Sanger sequencing, a novel mutation (c.26G>A) in *IRF6* (GenBank: NM_006147.3) was identified as the candidate aetiological variant. The variant replaced the arginine (Arg) at the ninth residue, which is a conserved site in multiple-sequence alignment, with glutamine (Gln), which affected the structure and function of IRF6 based on our modelling and prediction studies.

In the recruited family, the proband (D1) is affected by a cleft palate and lip, and another affected individual (D2) has a cleft lip only. The undiscovered subclinical phenotypes may be a possible illustration of the different phenotypes caused by one variant. Dixon *et al.* (1) thought that the phenotypic spectrum of non-syndromic CLP is more complex than previously realised and should include a variety of subclinical phenotypic features observed in either an individual with CLP and/or their 'unaffected' relatives (19). Defects of the orbicularis oris muscle is one of the subclinical phenotypes that can only be assessed using high-resolution ultrasound of the upper lip. It is a minor structural variant that we could not recognise when we recruited the family. However, if the affected mother (D2) has the subclinical phenotype, the different phenotypes of the proband (D1) and D2 would not be a qualitative difference, and the causative gene *IRF6* would be easily understood.

Moreover, different phenotypes might be caused by the same mutation. Basha *et al.* reported two NSCLP pedigrees shared a same mutation in *GRHL3* (p.Arg391Cys). But the affected members had different phenotypes, including CL/P, submucous cleft palate, velopharyngeal insuf ciency and/or hypernasal speech (20).

Variants in *IRF6* were consistently associated with NSCLP (21–23), including GWAS and candidate gene studies (5,12,13,24). An examination of sequence conservation across multiple species to identify *cis*-regulatory elements combined with an analysis of animal

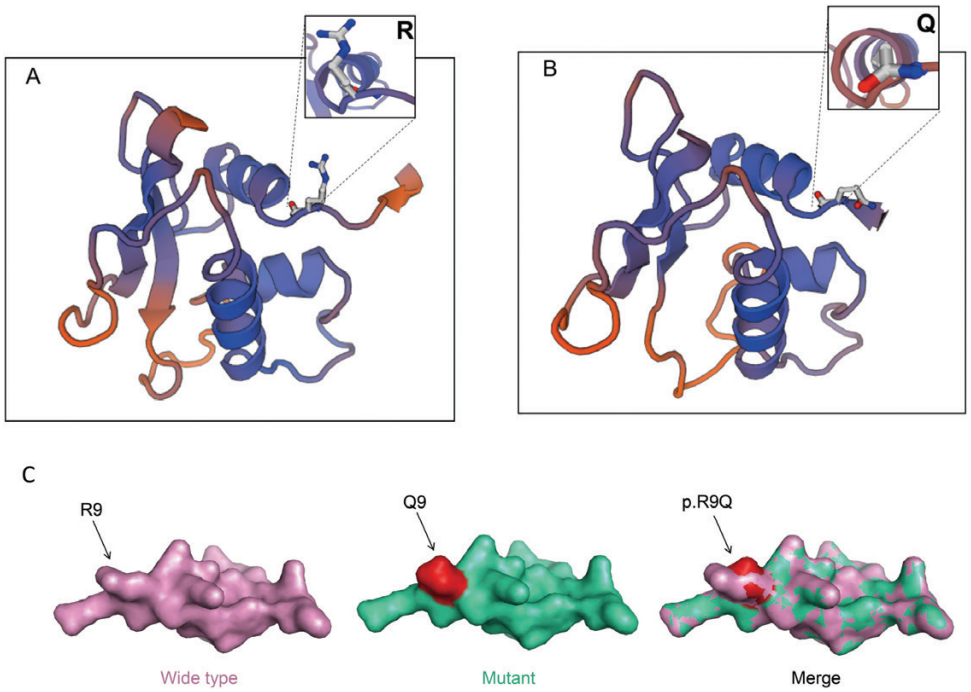

Figure 4. Homology models of the (**A**) wild-type and (**B**) mutant DBDs. The p.Arg9Gln variant replaces a positively charged amino acid with a very large neutral amino acid. The attraction of negative phosphates is lost. The wild-type residue sidechain is shown in the inset on the left, and the mutant sidechain in the inset on the right. The large sidechain of tryptophan will interfere with DNA molecules. (**C**) Altered electron-density distribution in merged models.

models and biochemical analyses resulted in the identification of one specific sequence variant (rs642961, located within an enhancer ~10 kb upstream of the *IRF6* transcription start site) that is significantly over-transmitted in non-syndromic cleft lip only (22). This apparent risk allele was found to disrupt a binding site for transcription factor AP2α, which is mutated in the autosomal-dominant CLP disorder branchio–oculo–facial syndrome (25), strongly suggesting that this SNP is a contributory variant (22).

The expression patterns indicate that *IRF6* not only plays a role in OFC-related tissue development but also in palatal fusion. According to the EMAGE database (www.embase.com), *IRF6* is strongly expressed in the developing maxillary process, lower jaw molar, oral epithelium, naris, upper jaw incisor, and molar. Sectional in situ hybridisation reveals expression of *IRF6* in the periderm of wild-type mouse embryos at E12, with a similar pattern being observed in the multilayered epidermis at E14 (26).

Animal models further supported the role of *IRF6* in CLP. *IRF6* mutant mice have a hyperproliferative epidermis that fails to undergo terminal differentiation, leading to multiple epithelial adhesions that can occlude the oral cavity and result in cleft palate (27,28). These results demonstrated that IRF6 is a key determinant of the keratinocyte proliferation–differentiation switch and plays a key role in formation of the oral periderm, whose spatiotemporal regulation is essential for ensuring appropriate palatal adhesion (29). A combination of mouse genetics, gene expression analyses, chromatin immunoprecipitation studies, and luciferase reporter assays has demonstrated that *IRF6* is a direct target of p63, which underlies several malformation syndromes that include CLP (30,31). p63 activates *IRF6* transcription via the *IRF6* enhancer element, and variation in this element increases the susceptibility to cleft lip only (32).

Recent studies have disclosed that IRF6 has functional interactions with other signalling pathways, such as regulating periderm differentiation and craniofacial development. Kwa *et al.* (33,34) reported receptor-interacting protein kinase 4 (*RIPK4*) promotes keratinocyte differentiation, in part, by inducing *IRF6* transactivator function through the phosphorylation of its C-terminal domain at Ser413 and Ser424; *SPRY4* signalling, included in receptor tyrosine kinase (*RTK*) signalling pathways, also interacts with *IRF6* in periderm development (35). Fakhouri *et al.* (36) reported that TWIST1 binds to the *IRF6* enhancer element and negatively suppresses its expression during craniofacial formation. Carpinelli *et al.* (37) thought grainyhead-like transcription factor 3 could promote periderm and palatal epithelial differentiation, particularly via interactions with IRF6.

Khandelwal *et al.* (2) performed targeted multiplex sequencing using molecular inversion probes (MIPs) in 1072 syndromic OFC patients, 67 tooth agenesis patients, and 706 controls. They identified three potentially pathogenic *de novo* mutations in OFC patients: Pro380Gln, Asp225His, and Arg9Trp in IRF6. We also identified a variant in the ninth residue, which in our case was a change from Arg to Gln. These results demonstrate the vital influence of the ninth position in NSCLP.

In our family, the mutation caused a structural alteration in the first domain, including a reduction in the distance between the first beta sheet and first alpha helix, an orientation alteration of the residue side chain and a change in electron-density distribution. All of these would affect the function of DNA binding. IRF6 belongs to a transcription factor family, and the structural changes may influence the binding of DNA and interfere with downstream transcription. The downstream target genes including *KLF4* (38) and *GRHL3* (39), which would regulate oral periderm differentiation, and *SNAI2* (40), which is involved in the regulation of epithelial mesenchymal transition and palatal fusion, could be affected. Therefore, the mutation may affect downstream functions such as keratinocyte proliferation and differentiation and eventually lead to CLP (26–28).

In conclusion, our data suggest that rare *IRF6* variants play a role in the aetiology of NSCLP, although the pathogenic mechanism of *IRF6* is not completely understood and requires further exploration using other techniques, such as animal models and cellular and molecular experiments. Our study highlights the need for further exploration of unknown variants in *IRF6*, which may contribute to our understanding of the aetiology and prevention of NSCLP.

Supplementary data

Supplementary Tables 1 and 2 are available at *Mutagenesis* Online.

Funding

This work was supported by the Beijing Municipal Natural Science Foundation (7182184) and the Interdisciplinary Medicine Seed Fund of Peking University (BMU2017MB006).

Acknowledgements

We thank the family participating in this study. We thank the reviewers for their critical and insightful suggestions about our work.

Conflict of interest statement: None declared.

References

1. Dixon, M. J., Marazita, M. L., Beaty, T. H. and Murray, J. C. (2011) Cleft lip and palate: understanding genetic and environmental influences. *Nat. Rev. Genet*., 12, 167–178.
2. Khandelwal, K. D., Ishorst, N., Zhou, H., *et al.* (2017) Novel IRF6 mutations detected in orofacial cleft patients by targeted massively parallel sequencing. *J. Dent. Res*., 96, 179–185.
3. Yu, Y., Zuo, X., He, M., *et al.* (2017) Genome-wide analyses of non-syndromic cleft lip with palate identify 14 novel loci and genetic heterogeneity. *Nat. Commun*., 8, 14364.
4. Sun, Y., Huang, Y., Yin, A., *et al.* (2015) Genome-wide association study identifies a new susceptibility locus for cleft lip with or without a cleft palate. *Nat. Commun*., 6, 6414.
5. Birnbaum, S., Ludwig, K. U., Reutter, H., *et al.* (2009) Key susceptibility locus for nonsyndromic cleft lip with or without cleft palate on chromosome 8q24. *Nat. Genet*., 41, 473–477.
6. Wu, D., Mandal, S., Choi, A., *et al.* (2015) DLX4 is associated with orofacial clefting and abnormal jaw development. *Hum. Mol. Genet*., 24, 4340–4352.
7. Tian, H., Feng, J., Li, J., *et al.* (2017) Intraflagellar transport 88 (IFT88) is crucial for craniofacial development in mice and is a candidate gene for human cleft lip and palate. *Hum. Mol. Genet*., 26, 860–872.
8. Ingraham, C. R., Kinoshita, A., Kondo, S., *et al.* (2006) Abnormal skin, limb and craniofacial morphogenesis in mice deficient for interferon regulatory factor 6 (Irf6). *Nat. Genet*., 38, 1335–1340.
9. Peyrard-Janvid, M., Leslie, E. J., Kousa, Y. A., *et al.* (2014) Dominant mutations in GRHL3 cause Van der Woude Syndrome and disrupt oral periderm development. *Am. J. Hum. Genet*., 94, 23–32.
10. Bureau, A., Parker, M. M., Ruczinski, I., *et al.* (2014) Whole exome sequencing of distant relatives in multiplex families implicates rare variants in candidate genes for oral clefts. *Genetics*, 197, 1039–1044.
11. Burdick, A. B. (1986) Genetic epidemiology and control of genetic expression in van der Woude syndrome. *J. Craniofac. Genet. Dev. Biol. Suppl*., 2, 99–105.
12. Grant, S. F., Wang, K., Zhang, H., *et al.* (2009) A genome-wide association study identifies a locus for nonsyndromic cleft lip with or without cleft palate on 8q24. *J. Pediatr*., 155, 909–913.
13. Mangold, E., Ludwig, K. U., Birnbaum, S., *et al.* (2010) Genome-wide association study identifies two susceptibility loci for nonsyndromic cleft lip with or without cleft palate. *Nat. Genet*., 42, 24–26.
14. Chen, Y., Chen, Y., Shi, C., *et al.* (2018) SOAPnuke: a MapReduce acceleration-supported software for integrated quality control and preprocessing of high-throughput sequencing data. *GigaScience*, 7, 1–6.
15. Adzhubei, I. A., Schmidt, S., Peshkin, L., Ramensky, V. E., Gerasimova, A., Bork, P., Kondrashov, A. S. and Sunyaev, S. R. (2010) A method and server for predicting damaging missense mutations. *Nat. Methods*, 7, 248–249.
16. Biasini, M., Bienert, S., Waterhouse, A., *et al.* (2014) SWISS-MODEL: modelling protein tertiary and quaternary structure using evolutionary information. *Nucleic Acids Res*., 42, W252–W258.
17. Murray, J. C. (2002) Gene/environment causes of cleft lip and/or palate. *Clin. Genet*., 61, 248–256.
18. Khandelwal, K. D., van Bokhoven, H., Roscioli, T., Carels, C. E. and Zhou, H. (2013) Genomic approaches for studying craniofacial disorders. *Am. J. Med. Genet. C. Semin. Med. Genet*., 163C, 218–231.
19. Weinberg, S. M., Naidoo, S. D., Bardi, K. M., Brandon, C. A., Neiswanger, K., Resick, J. M., Martin, R. A. and Marazita, M. L. (2009) Face shape of unaffected parents with cleft affected offspring: combining three-dimensional surface imaging and geometric morphometrics. *Orthod. Craniofac. Res*., 12, 271–281.
20. Basha, M., Demeer, B., Revencu, N., *et al.* (2018) Whole exome sequencing identifies mutations in 10% of patients with familial non-syndromic cleft lip and/or palate in genes mutated in well-known syndromes. *J. Med. Genet*., 55, 449–458.
21. Ghassibé, M., Bayet, B., Revencu, N., Verellen-Dumoulin, C., Gillerot, Y., Vanwijck, R. and Vikkula, M. (2005) Interferon regulatory factor-6: a gene predisposing to isolated cleft lip with or without cleft palate in the Belgian population. *Eur. J. Hum. Genet*., 13, 1239–1242.
22. Rahimov, F., Marazita, M. L., Visel, A., *et al.* (2008) Disruption of an AP-2alpha binding site in an IRF6 enhancer is associated with cleft lip. *Nat. Genet*., 40, 1341–1347.
23. Zucchero, T. M., Cooper, M. E., Maher, B. S., *et al.* (2004) Interferon regulatory factor 6 (*IRF6*) gene variants and the risk of isolated cleft lip or palate. *N. Engl. J. Med*., 351, 769–780.
24. Beaty, T. H., Murray, J. C., Marazita, M. L., *et al.* (2010) A genome-wide association study of cleft lip with and without cleft palate identifies risk variants near *MAFB* and *ABCA4*. *Nat. Genet*., 42, 525–529.
25. Milunsky, J. M., Maher, T. A., Zhao, G., *et al.* (2008) TFAP2A mutations result in branchio-oculo-facial syndrome. *Am. J. Hum. Genet*., 82, 1171–1177.
26. Richardson, R. J., Hammond, N. L., Coulombe, P. A., *et al.* (2014) Periderm prevents pathological epithelial adhesions during embryogenesis. *J. Clin. Invest*., 124, 3891–3900.
27. Richardson, R. J., Dixon, J., Malhotra, S., Hardman, M. J., Knowles, L., Boot-Handford, R. P., Shore, P., Whitmarsh, A. and Dixon, M. J. (2006) Irf6 is a key determinant of the keratinocyte proliferation-differentiation switch. *Nat. Genet*., 38, 1329–1334.
28. Ingraham, C. R., Kinoshita, A., Kondo, S., *et al.* (2006) Abnormal skin, limb and craniofacial morphogenesis in mice deficient for interferon regulatory factor 6 (IRF6). *Nat. Genet*., 38, 1335–1340.
29. Richardson, R. J., Dixon, J., Jiang, R. and Dixon, M. J. (2009) Integration of *IRF6* and *Jagged2* signalling is essential for controlling palatal adhesion and fusion competence. *Hum. Mol. Genet*., 18, 2632–2642.
30. Celli, J., Duijf, P., Hamel, B. C., *et al.* (1999) Heterozygous germline mutations in the *p53* homolog *p63* are the cause of EEC syndrome. *Cell*, 99, 143–153.
31. McGrath, J. A., Duijf, P. H., Doetsch, V., *et al.* (2001) Hay-Wells syndrome is caused by heterozygous missense mutations in the SAM domain of p63. *Hum. Mol. Genet*., 10, 221–229.
32. Thomason, H. A., Zhou, H., Kouwenhoven, E. N., *et al.* (2010) Cooperation between the transcription factors *p63* and *IRF6* is essential to prevent cleft palate in mice. *J. Clin. Invest*., 120, 1561–1569.
33. Kwa, M. Q., Huynh, J., Reynolds, E. C., Hamilton, J. A. and Scholz, G. M. (2015) Disease-associated mutations in IRF6 and RIPK4 dysregulate their signalling functions. *Cell. Signal*., 27, 1509–1516.
34. Kwa, M. Q., Huynh, J., Aw, J., Zhang, L., Nguyen, T., Reynolds, E. C., Sweet, M. J., Hamilton, J. A. and Scholz, G. M. (2014) Receptor-interacting protein kinase 4 and interferon regulatory factor 6 function as a signaling axis to regulate keratinocyte differentiation. *J. Biol. Chem*., 289, 31077–31087.

35. Kousa, Y. A., Roushangar, R., Patel, N., Walter, A., Marangoni, P., Krumlauf, R., Klein, O. D. and Schutte, B. C. (2017) *IRF6* and *SPRY4* signaling interact in periderm development. *J. Dent. Res*., 96, 1306–1313.
36. Fakhouri, W. D., Metwalli, K., Naji, A., Bakhiet, S., Quispe-Salcedo, A., Nitschke, L., Kousa, Y. A. and Schutte, B. C. (2017) Intercellular genetic interaction between IRF6 and Twist1 during craniofacial development. *Sci. Rep*., 7, 7129.
37. Carpinelli, M. R., de Vries, M. E., Jane, S. M. and Dworkin, S. (2017) Grainyhead-like transcription factors in craniofacial development. *J. Dent. Res*., 96, 1200–1209.
38. Liu, H., Leslie, E. J., Jia, Z., Smith, T., Eshete, M., Butali, A., Dunnwald, M., Murray, J. and Cornell, R. A. (2016) *Irf6* directly regulates *Klf17* in zebrafish periderm and *Klf4* in murine oral epithelium, and dominant-negative *KLF4* variants are present in patients with cleft lip and palate. *Hum. Mol. Genet*., 25, 766–776.
39. de la Garza, G., Schleiffarth, J. R., Dunnwald, M., *et al*. (2013) Interferon regulatory factor 6 promotes differentiation of the periderm by activating expression of Grainyhead-like 3. *J. Invest. Dermatol*., 133, 68–77.
40. Ke, C. Y., Xiao, W. L., Chen, C. M., Lo, L. J. and Wong, F. H. (2015) IRF6 is the mediator of TGFβ3 during regulation of the epithelial mesenchymal transition and palatal fusion. *Sci. Rep*., 5, 12791.